International Journal of Nanomedicine

Dovepress
open access to scientific and medical research

Open Access Full Text Article

ORIGINAL RESEARCH

High Efficacy Combined Microneedles Array with Methotrexate Nanocrystals for Effective Anti-Rheumatoid Arthritis

Fang Wei[1], Qiuyue Wang[1], Hang Liu[1], Xuejing Yang[1], Wenyu Cao[1], Weiman Zhao[1], Yingying Li[1], Lijie Zheng[1], Tao Ma[1,2], Qingqing Wang[1–3]

[1]School of Pharmacy, Bengbu Medical College, Bengbu, Anhui Province, 233030, People's Republic of China; [2]Engineering Research Center for Biochemical Pharmaceuticals of Anhui Province, Bengbu Medical College, Bengbu, Anhui Province, 233030, People's Republic of China; [3]Bengbu BBCA Medical Science Co., Ltd., Bengbu, Anhui Province, 233030, People's Republic of China

Correspondence: Qingqing Wang; Tao Ma, School of Pharmacy, Bengbu Medical College, Bengbu, Anhui Province, 233030, People's Republic of China, Tel +86 15605528300; +86 13855266592, Email qingqingwang@bbmc.edu.cn; matao1992@foxmail.com

Introduction: Methotrexate (MTX) is the first-line drug for the treatment of rheumatoid arthritis (RA) in several countries. However, MTX has an extremely low solubility in water, and the side effects caused by its delivery mode restrict its curative effect. In this study, we designed a dissolving microneedles array (DMNA) containing MTX nanocrystals (MTX-NCs) (MTX-NC@DMNA) to improve the treatment of RA. DMNA-based drug delivery combines the advantages of patient compliance with the use of transdermal drug delivery systems and high-efficiency injection administration; thus, it can mitigate the side effects that result from current administration routes. Carrier-free and surfactant-free MTX-NCs were prepared to overcome bioavailability limitations and poor drug loading problems.

Methods: The MTX-NCs prepared by reverse solvent precipitation method was encapsulated in the DMNA. The morphology, mechanical properties, safety, stability and in vivo dissolution were evaluated, and its pharmacodynamic characteristics were assessed in a rat model of RA.

Results: The particle size of the MTX-NCs was 148.1 ± 10.1 nm. The MTX-NC@DMNA were found to be rigid enough to penetrate the skin and deliver the drug successfully. The results indicated effective skin recovery after removal of the DMNA. It was found that the MTX-NC@DMNA significantly reduced foot swelling in the rats and regulated the balance in the levels of related cytokines. It also reduced pathological damage to the synovium, joint, and cartilage, and effectively alleviated organ injury in the rats.

Conclusion: Transdermal administration of MTX-NC@DMNA may be an effective approach for treating RA.

Keywords: nanocrystals, inflammation, dissolving microneedles array, transdermal, rheumatoid arthritis

Introduction

Rheumatoid arthritis (RA) is a systemic and chronic autoimmune disease.[1,2] Its main pathological features include proliferation of synovial lining cells, many inflammatory cells in the stroma, proliferation of microvessels, formation of pannus, and destruction of cartilage and bone structure, which can result in joint deformity and loss of function. Consequently, patients with RA experience great pain and suffering.[3–5]

At present, there are several drugs for the clinical treatment of RA, which include non-steroidal anti-inflammatory drugs, glucocorticoids, and disease-modifying antirheumatic drugs.[6] Methotrexate (MTX) is an antirheumatic drug that can continuously alleviate the symptoms of RA, inhibit progressive damage to tissues and joints, and delay or prevent the development of the disease. It has been widely used in the clinical treatment of RA.[7–9]

The main dosage forms of MTX that are used clinically are tablets and injections.[10–13] Long-term oral administration of MTX can result in adverse reactions such as digestive tract problems,[14,15] myelosuppression,[16,17] and abnormal liver and kidney function.[18,19] Moreover, MTX injection must be administered by healthcare professionals and the needles used are

Received: 21 March 2022
Accepted: 13 May 2022
Published: 24 May 2022

Graphical Abstract

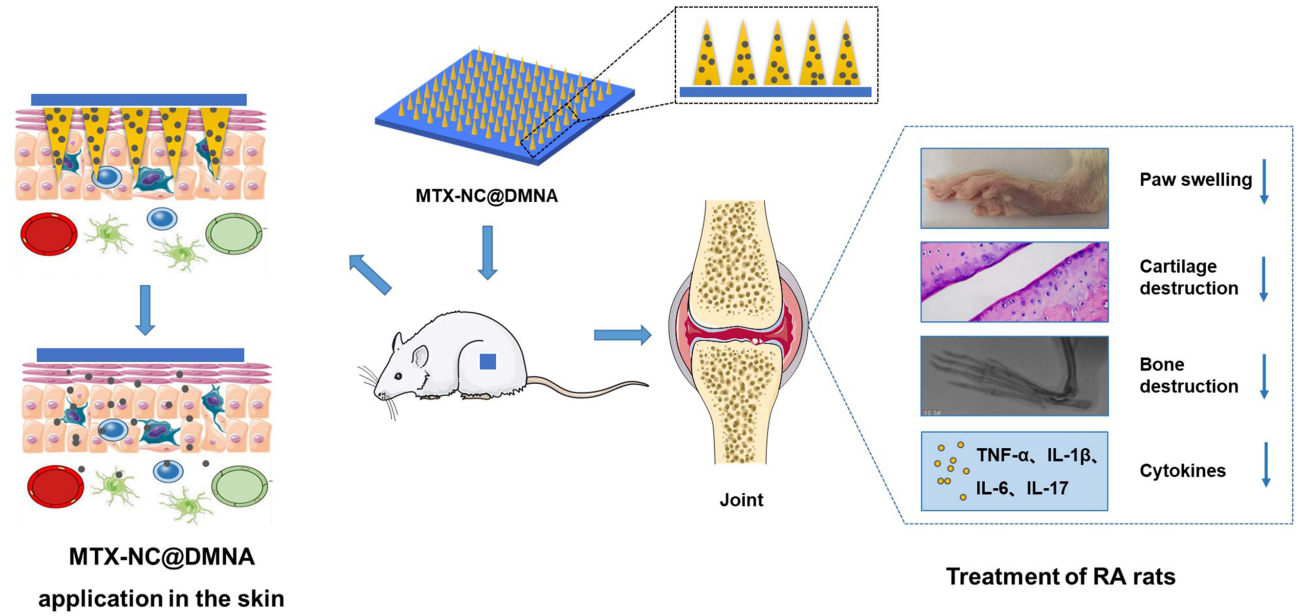

a biohazard. The injection is also inconvenient for patients and can cause pain and bleeding.[20–23] Therefore, to overcome the above shortcomings associated with the administration of MTX tablets and injections, it is necessary to develop a new dosage form that can be administered via an alternative route.

The dissolving microneedles array (DMNA)[24–26] is composed of water-soluble and active drugs. After administration, microneedles (MNs) inserted into the skin dissolve rapidly to efficiently release the drug they contain. This mode of drug administration is effective and can be used to achieve the same delivery efficiency of an injection. It can also avoid the damage to rich nerve endings and capillaries in the dermis by larger needles,[27,28] which can reduce or eliminate pain and infection. Additionally, the use of a DMNA is associated with patient compliance and convenience of administration as the use of a transdermal patch is. Therefore, combining the advantages of injection and transdermal drug administration, while avoiding their disadvantages, DMNA-based drug delivery may be a promising method of drug delivery for the treatment of RA.

MTX is poorly soluble in water, which affects its bioavailability and can have a critical impact on its loading into formulations, especially DMNA, which are expected to solve problems related to MTX delivery. The characteristics of DMNA as well as the process for their preparation indicate that to ensure adequate drug loading, the drug to be incorporated in the formulation must have a high-water solubility.

Drugs that are insoluble in water can be prepared as nanocrystals (NCs), also known as nanosuspensions, in order to formulate them as "pure" nano-drug delivery systems. The particle size of NCs is less than 1 μm, usually 100−500 nm.[29–32] The solubility characteristics of drugs change as particle size decreases to the nanometer scale, which leads to a significant increase in dissolution rate. As a result, drug NCs show some unique properties with respect to biopharmaceutics. Drugs that are insoluble in water can show improved solubility and dissolution characteristics when they are prepared as NCs. Compared to other delivery systems such as liposomes and hydrogel,[33] NCs do not need any carriers, which greatly improves drug loading and safety. Therefore, NCs are a useful solution for overcoming bioavailability limitations and poor drug loading problems. Although the NC is a "carrier-free" system, surface-active agents are usually needed in their preparation to prevent aggregation of colloidal particles and thus improve stability;[34] however, this may also pose uncertain safety risks in vivo. Therefore, it is important to reduce or eliminate the use of surfactants during the preparation of NCs to further improve their effectiveness and safety.

In this study, we developed a DMNA drug delivery system loaded with MTX-NCs (MTX-NC@DMNA) for the treatment of RA. Surfactant-free MTX-NCs were prepared using the anti-solvent precipitation method, after which they were loaded into a DMNA system. The mechanical properties, skin insertion properties, and carrier dissolution profile of the DMNA were determined. The in vivo efficacy of the drug delivery system was also evaluated. Our results provide evidence for the potential use of MTX-NC@DMNA as an innovative drug delivery system for the treatment of RA.

Materials and Methods

The Animals Studies

Male Sprague-Dawley (SD) rats (weight, 180 g) were purchased from Jinan Pengyue Laboratory Animal Breeding Co., Ltd. (Jinan, China) (license no.: SCXK (LU) 20190003). All animal procedures comply with animal ethics requirements. The animal experimental procedure was approved by the Animal Care Committee of Bengbu Medical College (License No.: 2021040) on 10 March 2021 and conformed to the Animal Ethical Standards and Use Committee at Bengbu Medical College.

Cell Line and Culture

The murine macrophage cell line RAW264.7 was purchased from American Type Culture Collection (Manassas, VA, USA) for the study. The cells were cultured in Dulbecco's Modified Eagle Medium supplemented with 10% fetal bovine serum and 5% CO_2 at 37°C.

Fabrication of MTX-NCs

MTX-NCs were prepared using the anti-solvent precipitation method.[35] Initially, 0.125 g MTX was dispersed in 5 mL ultra-pure water. 0.55 mL Sodium hydroxide in a benign solvent (1 mol/L) was then added to the mixture to dissolve MTX completely. Under stirring (2000 g, on ice), 0.275 mL hydrochloric acid in a non-benign solvent (1 mol/L) was added to the mixture obtained to control particle formation. MTX-NCs suspension was obtained by further stirring the mixture for 1 h (2000 g, on ice).

Characterization of MTX-NCs

Physicochemical Characterization of MTX-NCs

The particle size, polydispersity index (PDI), and zeta potential of the MTX-NCs were measured using a particle size analyzer (Malvern Panalytical, Malvern, UK). The MTX-NCs suspension was diluted with pure water, after which its stability was determined. Each measurement was performed in triplicate. The morphology of the MTX-NCs was evaluated by scanning electron microscopy (SEM). The pH of the formulation was determined using a pH meter.

Determination of Drug Content and Saturation Solubility of MTX-NCs

To determine MTX loading in the MTX-NCs, adding sodium hydroxide solution in the NCs to completely dissolved it. The solution obtained was filtered using a 0.22 μm filter head, after which MTX amount was determined by high-performance liquid chromatography (HPLC).

To determine saturation solubility, excess lyophilized MTX-NCs powder and MTX were completely dissolved in 1 mL pure water and 1 mL phosphate-buffered saline (PBS), respectively. The solutions were then centrifuged at 15,000 *g* for 30 min and left to stand for 24 h. The supernatants were centrifuged at 15,000 *g* for 30 min, diluted, and analyzed by HPLC. A standard curve was plotted and used in the calculation of saturation solubility. Three parallel samples of each solution were analyzed.

The physical crystal state of the drug has an important influence on the solubility of the drug. In order to verify whether the crystal state of MTX changes during the preparation of MTX-NCs, powder X-ray diffraction (XRD) was used to confirm its structure. MTX, the auxiliary material (sodium chloride produced during preparation), a physical mixture of MTX and the auxiliary material, and the MTX-NCs were subjected to the XRD analysis.

In vitro Release of Drug

The in vitro release of MTX from the MTX-NCs was assessed using a dialysis method. Firstly, MTX (0.05 g) and MTX-NCs (containing 0.05 g MTX) were placed in dialysis membranes (8000–14,000 molecular weight cut-off), after which the membranes were placed in 500 mL PBS (37°C, 300 g). At predetermined times, 1 mL of the receiving solution was removed and replaced with 1 mL fresh PBS. Finally, the receiving solutions were filtered through 0.22 μm filter membranes, after which the filtrates were analyzed by HPLC. The release rate of MTX from each sample was then calculated using the following equation:

$$\%\ \text{Release} = \frac{\text{Total amount of actual release}}{\text{Total amount of drug}} \text{x}100\%$$

Stability Study of MTX-NCs

A Fourier-transform infrared (FTIR) spectrometer was used to investigate the chemical compositions of MTX and the MTX-NCs.

Physical stability was evaluated by storing the MTX-NCs at 4°C and 37°C in the dark for up to 42 days. Samples were taken at different time points for the assessment of particle size, PDI and zeta potential.

Fabrication of MTX-NC@DMNA

The prepared MTX-NCs were centrifuged at 14,500 *g* for 30 min to combine them with DMNA. The free drug in the supernatant were discarded, whereas NCs in the precipitate were used to prepare the MNs. To fabricate the DMNA, 200 mg HA was added to a 1 mL solution containing the MTX-NCs, followed by thorough mixing for 24 h. Second layer of PVP K90 aqueous solution (25 wt%).

The needle solution was poured into polydimethylsiloxane molds containing 10×10 lacunose arrays and centrifuged for 3 min at 3000 ×*g* (Thermo Electron LED GmbH, Osterode, Germany). After centrifugation, the molds were removed and the solution on their upper surfaces was scraped off. The molds were then left in a drying dish for 24 h. Next, 100 μL base solution was added to the molds, followed by centrifugation at 3000 ×*g* for 1 min. Thereafter, the molds were rotated 180° and centrifuged at 3000 ×*g* for 2 min. Immediately after centrifugation, the molds were placed in a drying oven and removed after they had dried at 37°C.

Characterization of MTX-NC@DMNA

The morphology of MTX-NC@DMNA was evaluated using a mobile microscope. The detailed surface morphology and dimensions of the DMNA were assessed by SEM.

The needle part of the MTX-NC@DMNA was cut off with a scalpel, adding sodium hydroxide solution to completely dissolved in 1mL pure water, and analyzed by HPLC.

The effect of MTX-NCs loading on the mechanical properties of the MNs was evaluated in this experiment. MTX-NC@DMNA and blank DMNA were prepared using the same method described above. The mechanical properties of the two DMNAs were evaluated using a texture analyzer. The back of each DMNA containing 100 MNs was placed on the cylindrical probe of the texture analyzer and secured in place with a double-sided adhesive, while ensuring that the tips were perpendicular to the stainless steel platform downward. During the experiment, the probe was moved onto a stainless steel platform at a speed of 2 mm/s. The probe detected pressure changes as the MNs touched the platform. When the trigger pressure reached 0.05 N, the probe changed speed to 0.5 mm/s and continued to move downward. The probe was then moved against the platform and away from the stainless steel platform, after which the MNs were removed for observation and measurement. Three DMNAs were selected and analyzed for each formulation, and at least 20 MN lengths were measured to calculate the average value. Mechanical strength was estimated as the percentage reduction in MN height after compression compared to the height before compression.

In vitro and in vivo Insertion Properties of MTX-NC@DMNA

To investigate the skin insertion property of the DMNA in vitro, excised SD rat skin was kept in normal saline for 30 min and then dried with filter paper for the study. MTX-NC@DMNA was inserted into the skin for 5 min and subsequently removed. The insertion site was stained with 0.4% trypan blue solution for 3 min, the residual trypan blue on the skin surface was wiped off, and the number of holes formed in the skin was observed under a microscope.

The skin insertion property of the DMNA was further studied in vivo. First, SD rats were anesthetized, after which their skin hair was shaved off. MTX-NC@DMNA was inserted into the skin for 5 min and subsequently removed, and the number of holes formed was observed under a microscope. The skin with the holes was then removed, fixed in 0.4% paraformaldehyde, embedded in paraffin, sliced, stained with hematoxylin and eosin (H&E), and observed under an optical microscope.

In vivo Dissolution of MTX-NC@DMNA

The dissolution of MTX-NC@DMNA in the skin of the rats was studied in this experiment. The rats were anesthetized and shaved, after which MTX-NC@DMNA was inserted into their skin for 2, 4, 6, 8, 10, 12 and 15 min. At the specified times, the MTX-NC@DMNA was removed and imaged using a microscope.

Safety Evaluation of MTX-NC@DMNA

Effects of Excipients on the Survival of RAW264.7 Cells

The 3-(4,5-dimethylthiazol-2-yl)-2,5-diphenyl tetrazolium bromide (MTT) method was used to assess the toxic effects of HA, PVP K90 and blank DMNA on RAW264.7 cells. Briefly, RAW264.7 cells (1×10^4) in the logarithmic growth phase were seeded into 96-well plates. When the cell density reached approximately 70%, the culture medium was replaced with a medium containing different concentrations of HA, PVP K90, or blank DMNA (5%,10%, 20% and 30%) solution. After incubating the plates for 24 h, cell viability was determined using the MTT assay.

Skin Recovery After MTX-NC@DMNA Insertion

Exposed dorsal rat skin was depilated and used in this experiment. MTX-NC@DMNA was inserted into the skin for 5 min and removed. The recovery process was recorded until micromoles on the skin were nearly invisible to the naked eye. A mobile microscope was used to take photographs of the skin before and at 0 min, 10 min, 20 min, 30 min, 1 h, 2 h and 3 h after insertion of the DMNA.

Pharmacodynamic Studies

Induction and Treatment of Adjuvant-Induced Arthritis in SD Rats

In this study, we aimed to investigate the pharmacodynamics of MTX-NC@DMNA in rats with adjuvant-induced arthritis. Complete Freund's adjuvant (CFA, 0.1 mL) was injected into the right hind footpad of the rats to induce RA. Starting on day 18 of the study, rats with RA were randomly divided into normal, model, MTX-NC@DMNA, MTX-NC @Cream, and oral MTX groups. The rats were administered the various test formulations every 3 days for 21 days. Rats in the MTX-NC@DMNA, MTX-NC@Cream, and oral MTX groups were treated with the respective formulations containing an equivalent of 200 μg MTX, whereas those in the normal and model groups were treated with equal volumes of normal saline.

Swelling of Rat Paw

Left hind paw volume was measured using a toe volume meter before (V_0) and every three days after (Vt) arthritis was induced in the rats. Paw swelling rate was estimated as a percentage using the following equation:

$$\text{Paw Swelling rate } (\%) = \frac{V_t}{V_0} \text{ x100\%}$$

Infrared Thermal Imaging

After drug administration, an infrared thermal imager was used to take pictures of the ankle joints of the rats. Changes in body surface temperature at the ankle joints were also recorded.

Radiological Examination

To evaluate the severity of periarticular soft tissue swelling and joint space narrowing, the animals were anesthetized with 10% chloral hydrate on day 42 after they were administered CFA. The left ankle joints and paws were subjected to radiographic examination.

Histological Examination of the Synovium and Ankle Joint

The rats were sacrificed after they were treated with the various formulations. The synovium and ankle of the left hind limb were fixed in 4% paraformaldehyde solution, embedded in paraffin and sectioned. The sections were stained with H&E and safranin O/fast green and observed under a microscope.

Assessment of Related Inflammatory Factors

After drug administration, blood was collected from the retro-orbital plexus of the rats into centrifuge tubes without heparin. After 4 h, the supernatants were centrifuged at 3000 rpm for 10 min. The layer formed on top of each serum sample was carefully drained, labeled, and stored at −20°C for testing. The levels of interleukin (IL)-4, IL-10, IL-6, IL-17, IL-1β, and tumor necrosis factor (TNF)-α were determined using ELISA kits according to the manufacturer's instructions.

Safety Evaluation

To assess the safety of the different dosage forms of MTX, the main organs of the rats (heart, liver, spleen, lungs, and kidneys) were removed, embedded in paraffin, stained with H&E, and examined. Images of the samples were taken using a microscope.

Statistical Analysis

All the data obtained have been presented as mean ± standard deviation. Statistical significance in the data between two groups was analyzed using unpaired Student's *t*-test, whereas differences in data among multiple groups were evaluated using one-way analysis of variance. All statistical calculations were performed using GraphPad Prism version 8.0.2 (GraphPad Software Inc., La Jolla, CA, USA). Differences in data were considered statistically significant at $P < 0.05$.

Results and Discussion

Physicochemical Characterization of MTX-NCs

Various methods were used to characterize the prepared NCs. Particle size, PDI, and zeta potential were determined using a Malvern particle size analyzer. As shown in Figure 1A, the average particle size of the MTX-NCs was 148.1 ± 10.1 nm, whereas the PDI was 0.152 ± 0.024. These indicate that the MTX-NCs had a small particle size and a relatively uniform dispersion. The zeta potential was found to be −47.2 ± 0.7 mV. The absolute value of the zeta potential is greater than 10, which indicates good particle stability.

The morphology of the MTX-NCs was evaluated by SEM. The micrographs obtained are shown in Figure 1B. The MTX-NCs appeared spherical, and their particle size in the images was consistent with that obtained from using the particle size analyzer. Additionally, the distribution of the MTX-NCs was uniform.

The benign and non-benign solvents used in this experiment are strong bases and strong acids; therefore, the pH of the MTX-NCs formulation is important for further applications. The results showed that the pH of the NCs was 6.35 ± 0.02. This value is close to neutral, which means that acid-base imbalances in skin tissue fluid after administration of the NCs can be effectively avoided. Moreover, the MTX-NCs may be safer to use compared to an MTX solution with improved MTX solubility as a result of increased alkalinity.

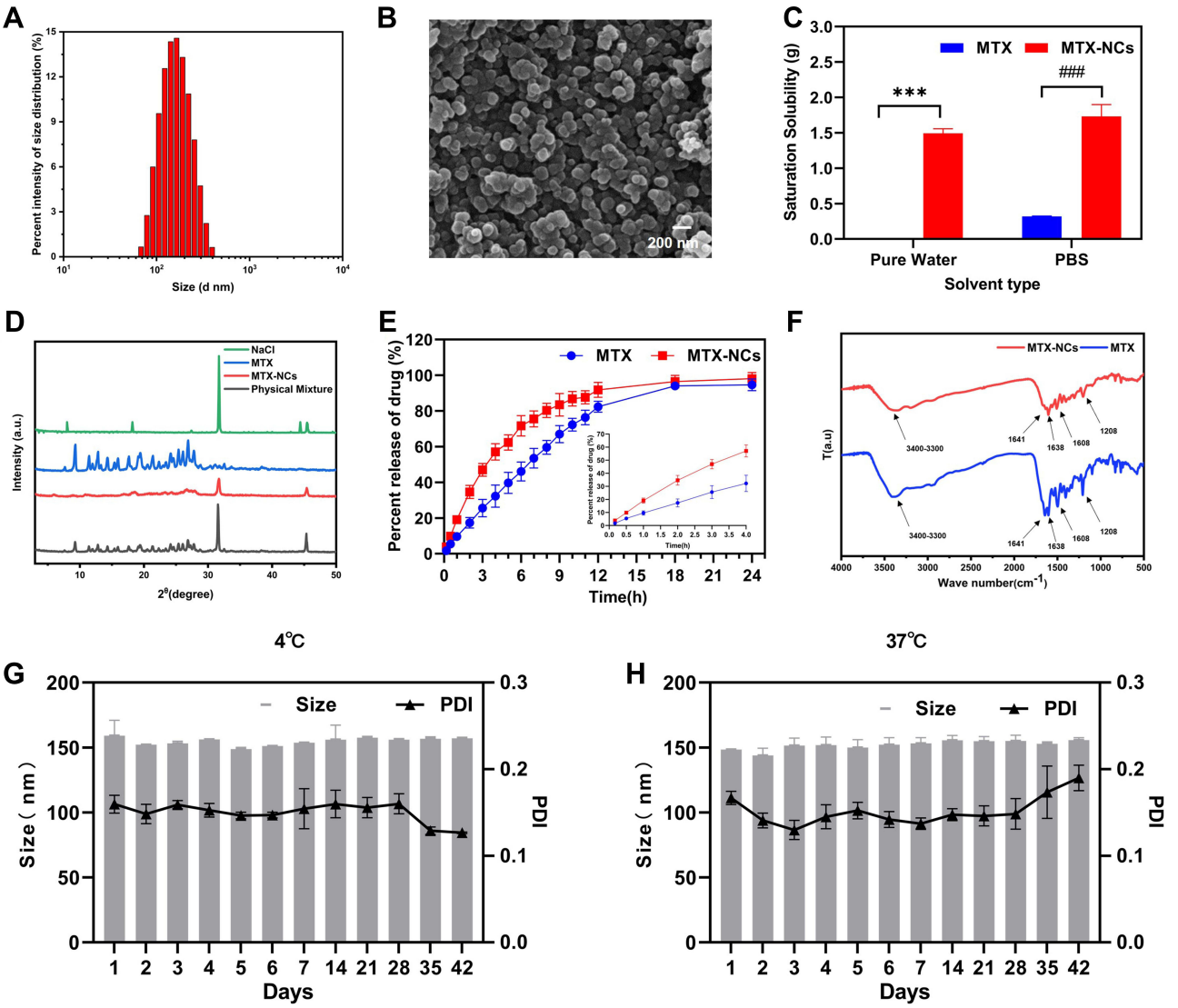

Figure 1 Results of MTX and MTX-NCs characterization. (**A**) Particle size of MTX-NCs. (**B**) SEM image of MTX-NCs. (**C**) Solubility of different dosage forms of MTX in different solvents. Data are presented as the mean ± SD (n = 3). ***$P < 0.001$ compared with the ratio of the saturated solubility of MTX in pure water. ###$P < 0.001$ compared with the ratio of the saturated solubility of MTX in PBS. (**D**) XRD patterns for NaCl, MTX, MTX-NCs and physical mixture of MTX and NaCl. (**E**) In vitro release curve of MTX from the different dosage forms. Data are presented as the mean ± SD (n = 3). (**F**) FTIR spectra of MTX-NCs and MTX. (**G**–**H**) Particle size and PDI of MTX-NCs at 4°C and 37°C. Data are presented as the mean ± SD (n = 3).

Abbreviations: MTX, methotrexate; MTX-NCs, MTX nanocrystals; SEM, scanning electron microscopy; PBS, phosphate-buffered saline; XRD, powder X-ray diffraction; NaCl, sodium chloride; FTIR, Fourier-transform infrared; PDI, polydispersity index.

MTX Content in the NCs and Saturation Solubility

The content of MTX in the MTX-NCs was high (94.8 ± 1.2%), indicating that NCs as carrier-free nanoparticles can significantly improve drug content.

After preparing the MTX-NCs, the saturated solubility in water and PBS increased 240.758 and 5.421 times, respectively (Figure 1C). The water solubility of MTX was also improved to varying degrees.

As shown in Figure 1D, the patterns for MTX and sodium chloride appeared as many groups of sharp peaks, indicating that they were crystals. Additionally, the characteristic peaks of MTX and sodium chloride were retained in the pattern for the physical mixture. The XRD pattern for the MTX-NCs was dispersed; however, the characteristic peak of sodium chloride was retained, indicating that after MTX was prepared into NCs, its crystalline state changed to an amorphous state. Therefore, the saturation solubility of MTX is significantly improved after NCs preparation.

In vitro Release of Drug

NCs can overcome the solubility and bioavailability problems of poorly soluble active pharmaceutical ingredients by enhancing dissolution rate and increasing supersaturated solubility. The differences between the MTX-NCs and MTX were studied in an in vitro drug release experiment. The results of the study are shown in Figure 1E. The release rate of MTX from the MTX-NCs was higher than that obtained for the MTX, especially during the first few hours of the experiment. The release rate obtained for the MTX-NCs was twice that obtained for MTX.

Stability Study of MTX-NCs

The chemical structures of MTX and MTX-NCs were also evaluated in this study. The FTIR spectra of MTX and the MTX-NCs are shown in Figure 1F. The FTIR spectrum of MTX indicated several absorptions due to the presence of several functional groups. The stretching vibration bands between 3400 cm^{-1} and 3300 cm^{-1} were due to the appearance of broad peaks for N-H and O-H groups. The characteristic band at 1638 cm^{-1} corresponded to the presence of C=C stretching vibration. Similarly, vibration bands in the region of 1641 cm^{-1} indicated that C=O stretching partially overlapped with the N-H band, which appeared at approximately 1608 cm^{-1}. The vibration band at 1208 cm^{-1} indicates C-N stretching. Importantly, these peaks were also observed in the spectrum for the MTX-NCs. Therefore, it can be explained that the chemical structure of MTX did not change after it was used to prepare the MTX-NCs.

Physical stability of the MTX-NCs formulation was evaluated under 4°C and 37°C storage conditions for 42 days (Figure 1G and H). It was found that both MTX-NCs samples stored at 4°C and 37°C maintained a particle size of approximately 150 nm within 42 days without any significant changes. The PDI values of the samples remained below 0.2. The results showed that the MTX-NCs prepared in this study have a good storage stability.

Morphology and Drug Content of MTX-NC@DMNA

MTX-NC@DMNA was prepared using a two-step needle preparation method. The morphology of the MNs was characterized using a microscope. As shown in Figure 2A–C, the MTX-NC@DMNA consisted of 100 (10 × 10) clearly arranged needles. The MNs were conical with a smooth and uniform appearance. The needles formed were good and a height of 800 μm and a base diameter of 300 μm. The drug content per MN was 217.7 ± 11.3 μg.

Mechanical and Insertion Properties of MTX-NC@DMNA

The compressed shapes of blank DMNA and MTX-NC@DMNA are shown in Figure 2D–F. The heights of MTX-NC @DMNA and the blank DMNA decreased by 19% and 17%, respectively; however, the difference in the heights of the two formulations was not statistically significant. Both DMNAs had similar mechanical properties, indicating that the MTX-NCs loading did not affect the mechanical properties of the DMNA.

We investigated whether the DMNA was rigid enough to penetrate the skin and deliver the loaded drug successfully. As shown in Figure 2G–I, obvious pores were observed after MTX-NC@DMNA was inserted into the rat skin in vitro and the skin was stained with trypan blue. Similarly, pores were observed in the skin of the rats after MTX-NC@DMNA insertion in the in vivo study. Moreover, since the MTX-NCs formulation is yellow in color, we easily observed it in the pores. Pathological evaluation of the skin sections after MTX-NC@DMNA insertion showed the formation of conical microchannel in the skin, which is important for effective drug delivery.

In vivo Dissolution of MTX-NC@DMNA

Successful drug release from a DMNA is highly dependent on the dissolution of the DMNA. Therefore, we investigated the dissolution behavior of MTX-NC@DMNA in the rat skin in vivo instead of in the excised skin. As shown in Figure 2J–K, the length of the needles was reduced to half of their initial length after 4 min of MTX-NC @DMNA insertion. However, the MTX-NC@DMNA was completely dissolved after 15 min. Rapid dissolution of MTX-NC@DMNA can promote effective drug delivery, reduce the time of drug administration, and improve patient compliance.

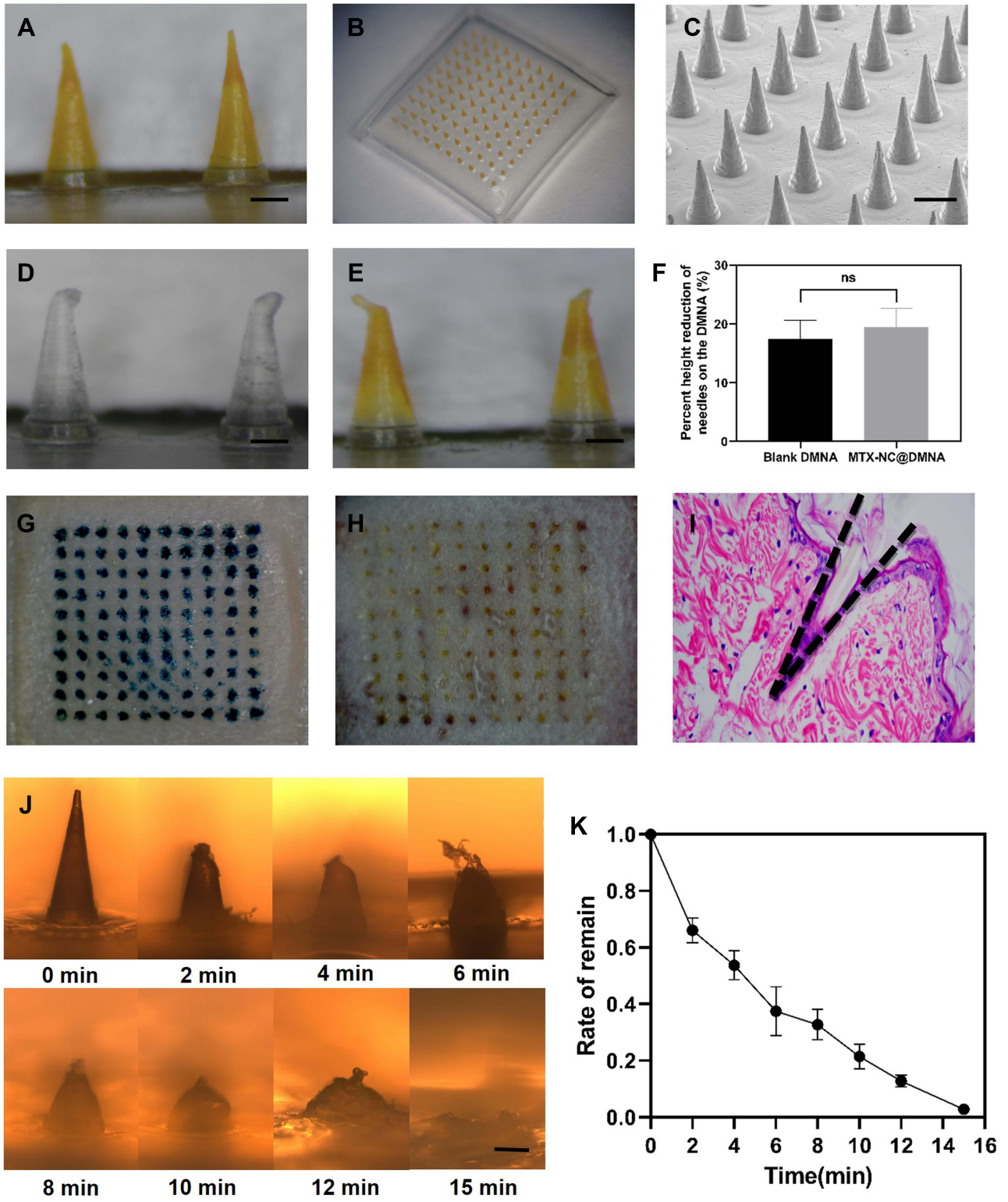

Figure 2 In vitro and in vivo studies on MTX-NC@DMNA. (**A**–**B**) Image of MTX-NC@DMNA. Scale bar = 200 μm. (**C**) SEM image of MTX-NC@DMNA. Scale bar = 500 μm. Images of (**D**) blank DMNA and (**E**) MTX-NC@DMNA after compression. Scale bar = 200 μm. (**F**) Percentage height reduction of needles on the DMNA prepared from the blank formulation and MTX-NCs. Data are presented as the mean ± SD (n = 20). Results of the insertion study for MTX-NC@DMNA (**G**) in vivo and (**H**) in vitro using rat skin. (**I**) Results of the H&E staining. (**J**) Image of MTX-NC@DMNA dissolution in vivo at different times. Scale bar = 200 μm. (**K**) MTX-NC@DMNA dissolution curve. Data are presented as the mean ± SD (n = 6).

Abbreviations: MTX-NC@DMNA, dissolving microneedles array containing MTX nanocrystals; SEM, scanning electron microscopy; DMNA, dissolving microneedles array; MTX-NCs, MTX nanocrystals; H&E, hematoxylin and eosin.

Safety Evaluation of MTX-NC@DMNA

Effects of the Excipients on the Survival of RAW264.7 Cells

The MTT method was used to investigate the cytotoxic effects of HA, PVP K90 and blank DMNA (5%, 10%, 20% and 30%) on the survival of RAW264.7 cells. As shown in Figure 3A, the growth rate of RAW264.7 cells reached approximately 100% after co-incubation with the three concentrations of HA, PVP K90 and blank DMNA solution for 24 h. There was no statistical difference in the data obtained. The results indicated that the excipients were safe and did not affect the growth of the cells.

Skin Recovery After MTX-NC@DMNA Insertion

The condition of the rat skin at the site of MTX-NC@DMNA insertion is shown in Figure 3B. There were obvious micropore arrays on the skin after removal of the DMNA. Over time, the pores gradually disappeared with the skin showing close to complete recovery after 3 h. No obvious sign of irritation such as erythema or swelling was observed during the observational period, indicating that the MN administration method was safe.

Pharmacodynamic Studies

Paw Swelling

The establishment of the RA model and the schematic diagram of the treatment plan are shown in Figure 4A.

Figure 4B shows changes in paw swelling rate from the beginning of model establishment to the end of the experiment. Paw swelling was observed after the establishment of the RA model in the rats. The results showed that the degree of swelling increased with time and reached a maximum value on day 27, after which it decreased slowly. After administration of the formulations, the degree of paw swelling was higher in the model group than in any of the other groups. Additionally, paw swelling in the MTX-NC@Cream group continued to increase slowly but decreased on day 27. However, paw swelling remained constant in the oral MTX group and then began to decrease on day 33. In contrast, it decreased significantly in the MTX-NC@DMNA group and further tended to decline in subsequent days. After the formulation administration period was over, there was no significant difference in paw swelling rate among the MTX-NC@Cream, oral MTX, and model groups. However, there was a significant difference in paw swelling rate between the MTX-NC@DMNA and model groups ($P < 0.5$), which indicated that MTX-NC@DMNA can effectively treat RA in rats.

Furthermore, after treatment administration, the groups that received MTX treatment were secondary to the lateral paw status (Figure 4C). Rats in the model group had significant paw swelling compared to those in the normal group. However, the groups treated with MTX showed different degrees of reduction in the swelling. Comparatively, the results for the MTX-NC@DMNA group were close to those obtained for the normal group, suggesting that MTX-NC@DMNA effectively reduces paw swelling in rats with RA.

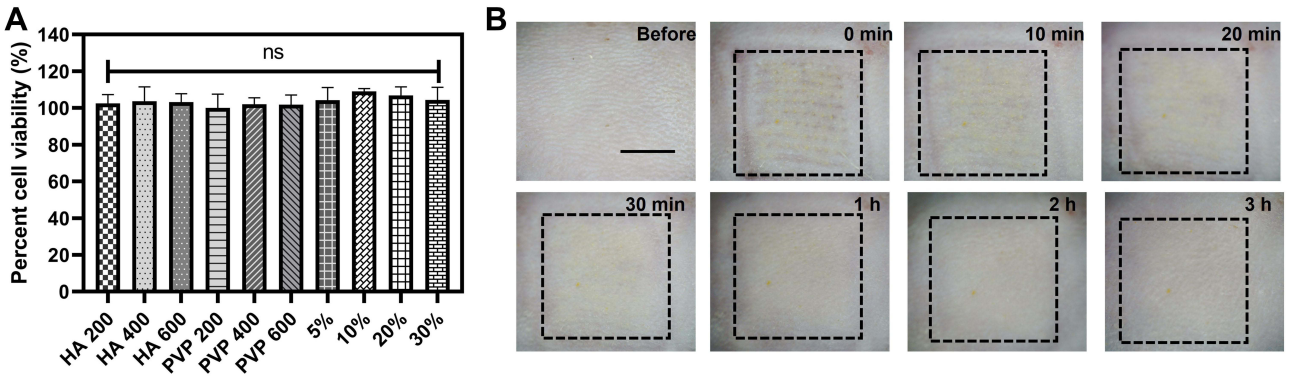

Figure 3 Safety evaluation of MTX-NC@DMNA. (**A**) Cytotoxicity test on excipients. Data are presented as the mean ± SD (n = 3). (**B**) Skin recovery after MTX-NC @DMNA insertion. Scale bar = 5 mm.

Abbreviations: HA, hyaluronic acid; PVP, polyvinyl pyrrolidone; MTX-NC@DMNA, dissolving microneedles array containing MTX nanocrystals.

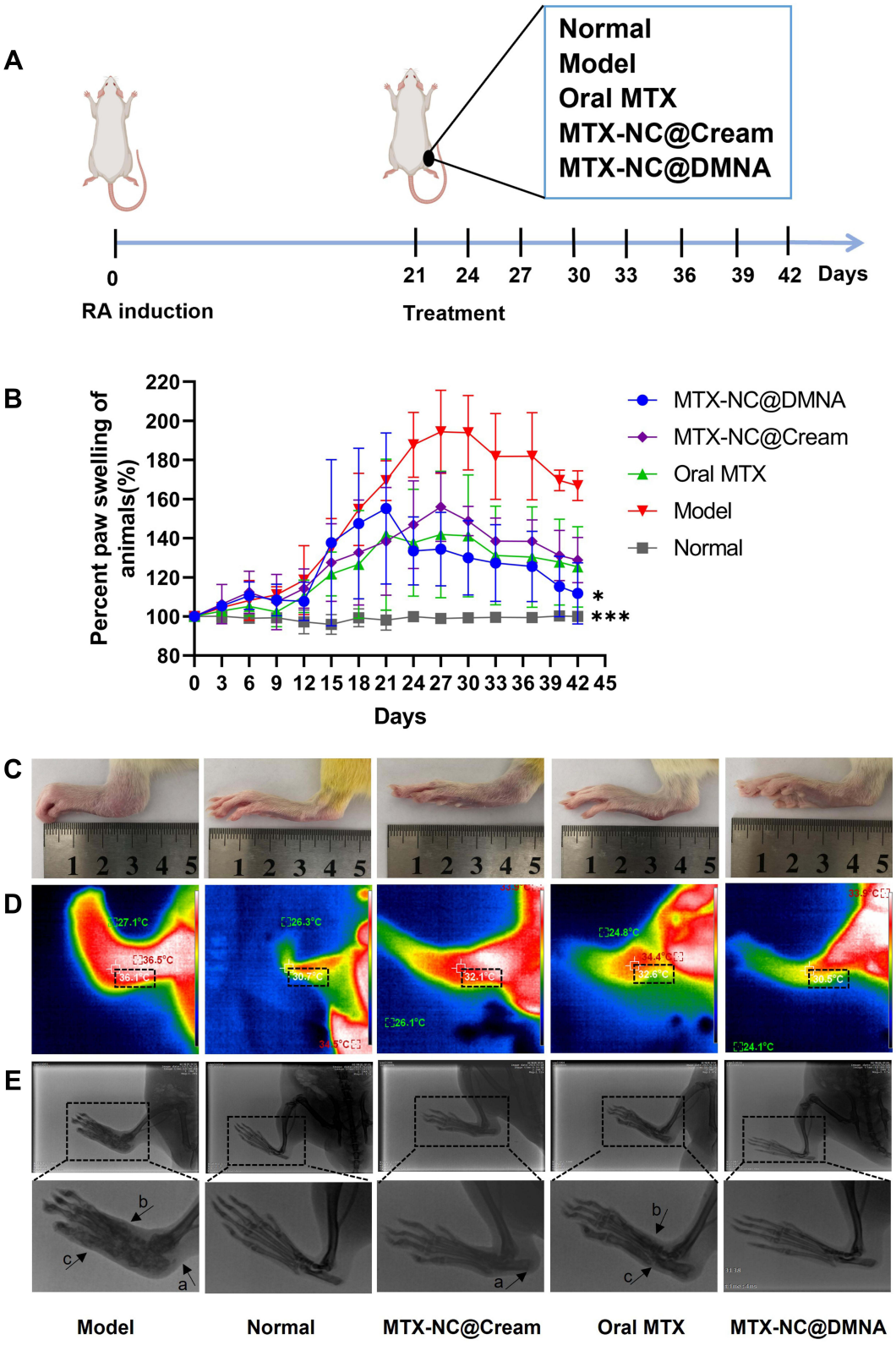

Figure 4 Evaluation of the effects of MTX-NC@DMNA in the rats. (**A**) Outline of efficacy assessment. (**B**) Changes in swelling rate in the rats. Data are presented as the mean ± SD (n = 6). ***$P < 0.001$ and *$P < 0.05$ compared with the model group. (**C**) Apparent state of the left hind paws of rats. (**D**) Thermal image of the left hind paws of the rats. (**E**) Radiological examination of different groups. a, soft tissue swelling; b, bone density reduction; c, bone defect.

Abbreviations: RA, rheumatoid arthritis; MTX, methotrexate; MTX-NC@DMNA, dissolving microneedles array containing MTX nanocrystals.

Infrared Thermal Imaging

The apparent pathological features of RA are redness, swelling, pain, and joint stiffness. The temperature at the ankle joint was measured by infrared thermal imaging to investigate inflammation in the different groups. Figure 4D shows that the ankle joint temperatures in the model, oral MTX, MTX-NC@Cream, MTX-NC@DMNA and normal groups were 36.1°C, 32.6°C, 32.1°C, 30.5°C and 30.7°C, respectively. The results indicate different degrees of relief among the groups. The temperature in the MTX-NC@DMNA group was the closest to that in the normal group. This indicates that MTX-NC@DMNA can effectively alleviate inflammation in RA, and that it can have a therapeutic effect in RA.

Radiological Examination

Rats in the various treatment groups were also subjected to radiological examination. As shown in Figure 4E, the model group showed severe soft tissue swelling, reduced local bone density, and bone defects. Additionally, there was significant improvement in secondary hind paw lesions in all the groups except the model group, indicating that MTX can alleviate the lesions and inflammation. More importantly, compared to the other treatment groups, rats in the MTX-NC@DMNA group had lower paw swelling, higher bone density, and fewer bone defects. These findings indicate that the secondary hind paw lesions in the MTX-NC@DMNA group were effectively relieved, and that MTX-NC@DMNA was superior to the other two MTX preparations.

Histological Examination of the Synovium and Ankle Joint

To confirm the therapeutic effect of MTX-NC@DMNA, joint tissue was stained with H&E and analyzed. The synovial tissue of rats in the model group showed abnormal hyperplasia accompanied by infiltration of inflammatory cells and pannus formation; however, these were not observed in the normal group (Figure 5A). Histopathological changes observed in the MTX-NC@Cream and oral MTX groups improved to some extent; however, marked pannus formation and inflammatory cell infiltration were still observed. The pathological state of the MTX-NC@DMNA group was similar to that of the normal group. MTX-NC@DMNA also had a better therapeutic effect than the other formulations had.

Results of the H&E staining of the ankle joint showed that the surface of the articular cartilage in the normal group was smooth, the cytoplasm was bright, and there was no inflammatory cell infiltration. In contrast, the untreated model group showed obvious exfoliation and inflammatory cell infiltration in the articular cavity. Furthermore, the cytoplasm was lighter in the MTX-NC@Cream group and the articular surface was uneven. There was inflammatory cell infiltration in the articular cavity in the oral MTX group; however, the articular surface in the MTX-NC@DMNA group was similar to that in the normal group, and the articular surface was flat with no inflammatory cell infiltration (Figure 5B). Similarly, safranin O/fast green staining of the ankle joint revealed that the normal group had a deeper stain, while the model group showed joint degeneration, light staining, and inflammatory cell infiltration. Compared to the model group, the MTX-NC@DMNA, MTX-NC@Cream, and oral MTX groups gradually showed a lighter stain. This suggests that MTX-NC@DMNA can effectively reduce synovial inflammation and joint injury in rats (Figure 5C).

Assessment of Related Inflammatory Factors

Cytokines are important factors that are involved in the development of joint synovitis and destruction of the articular cartilage and bone. ELISA kits were used to measure changes in cytokine levels in the study. We assessed the levels of anti-inflammatory (IL-4 and IL-10) and pro-inflammatory (TNF-α, IL-1β, IL-6 and IL-17) cytokines to evaluate the effects of the different formulations.

Changes in the levels of the anti-inflammatory cytokines are shown in Figure 5D–E. The serum levels of IL-4 and IL-10 were significantly lower in the model group than in the normal group ($P < 0.01$), indicating that the levels of anti-inflammatory factors decrease in RA. After treatment administration, the serum levels of IL-4 and IL-10 were found to be significantly lower in the MTX-NC@Cream and oral MTX groups than in the normal group, but similar in the MTX-NC@DMNA and normal groups. Additionally, serum IL-4 and IL-10 levels were significantly higher in the MTX-NC@DMNA group than in the model group ($P < 0.01$). These results suggest that MTX-NC@DMNA can increase the

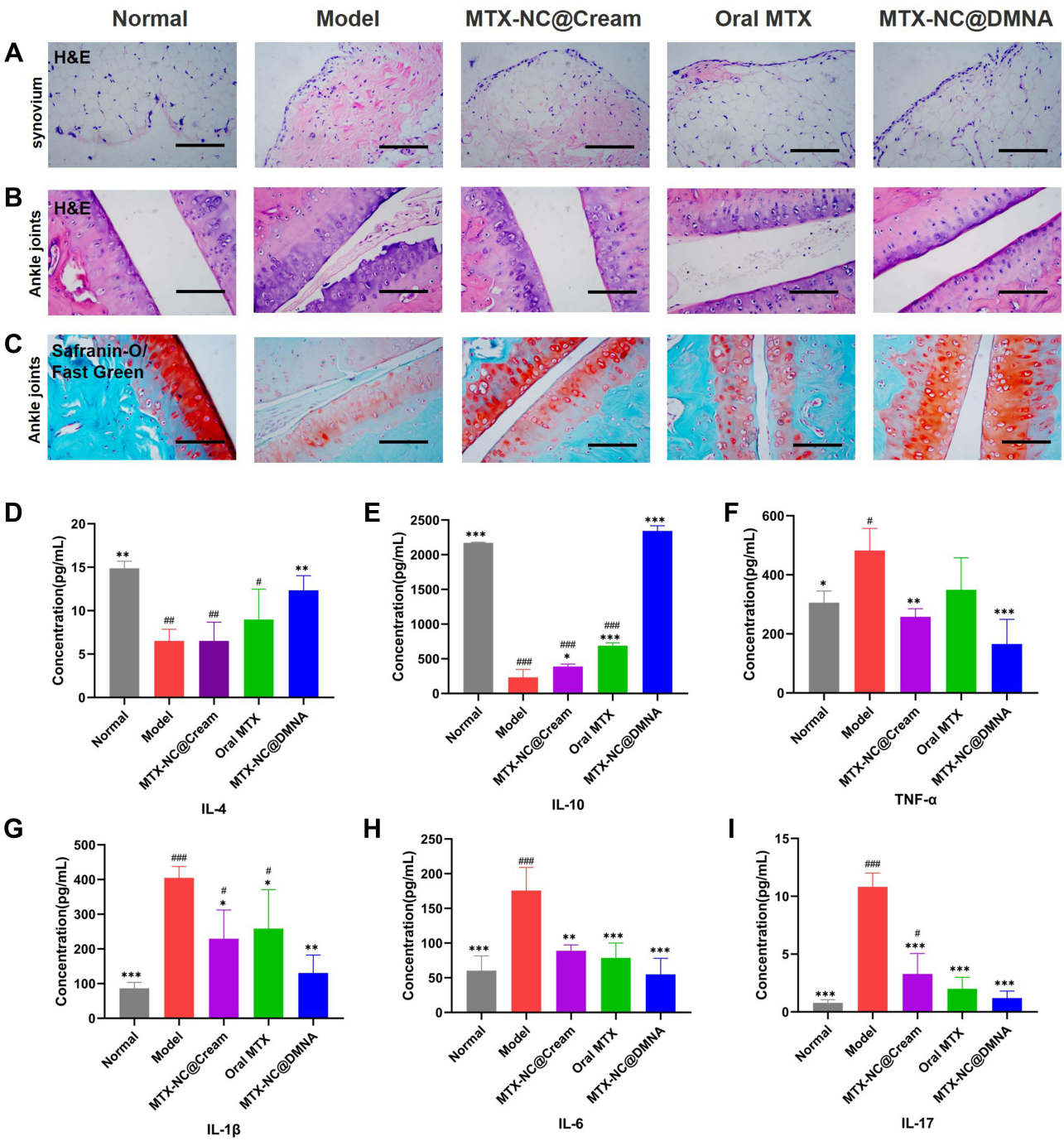

Figure 5 Histopathological changes in the (**A**) synovium and (**B**) ankle joints of the rats as assessed by H&E staining. (**C**) Histopathological changes in the ankle joints of the rats were assessed by safranin O/fast green staining. (**D**–**I**) Effects of MTX-NC@DMNA on the expression levels of cytokines in the serum of rats with RA. IL-4, IL-10, TNF-α, IL-1β, IL-6 and IL-17 levels were measured using ELISA kits. Data are presented as the mean ± SD (n = 3). $^{\#\#\#}P < 0.001$, $^{\#\#}P < 0.01$ and $^{\#}P < 0.05$ compared with the normal group. $^{***}P < 0.001$, $^{**}P < 0.01$ and $^{*}P < 0.05$ compared with the model group. Scale bar = 50 μm.

Abbreviations: H&E, hematoxylin and eosin; ELISA, enzyme linked immunosorbent assay; IL-4, interleukin-4; IL-10, interleukin-10; IL-6, interleukin-6; IL-17, interleukin-17; IL-1β, interleukin-1β; TNF-α, tumor necrosis factor-α.

serum levels of anti-inflammatory factors to their normal levels in rats with RA, and it has a significant advantage over the other two MTX formulations.

The levels of pro-inflammatory cytokines in the serum of the rats are shown in Figure 5F–I. The expression levels of TNF-α, IL-1β, IL-6 and IL-17 were significantly higher in the model group than in the normal group ($P < 0.05$),

indicating that RA development is accompanied by a significant increase in the levels of pro-inflammatory factors. Furthermore, the serum levels of TNF-α, IL-1β, IL-6 and IL-17 were lower to varying degrees in the MTX-treated groups than in the model group. The MTX-NC@DMNA formulation had the best effect on the levels of these cytokines, as the expression levels of all the pro-inflammatory factors were significantly decreased following the treatment with MTX-NC @DMNA ($P < 0.01$). These results show that MTX-NC@DMNA can effectively regulate the balance between pro-inflammatory and anti-inflammatory cytokine levels in rats. Additionally, it can alleviate systemic inflammatory responses as well as damage to articular cartilage and bone.

Safety Evaluation

To assess the safety of the different dosage forms of MTX, the major organs (including the heart, liver, spleen, lungs and kidneys) of the rats in each group were removed for H&E staining. As shown in Figure 6, in the normal group, the structure of cardiomyocytes was clear and myocardial fibers were slender. In the model group, myofibrils were unclear and interstitial edema was obvious. Pathological examination of the liver of normal rats revealed that the hepatic lobules were intact and hepatocytes were arranged radially around the central vein. In the model group, the structure of the hepatic cord was disordered and hepatocytes were slightly or moderately edematous. Additionally, the structure of the spleen in the normal group was clear, and the boundary between the white and red pulp was obvious. However, white and red pulps were blurred in the model group. There was a small amount of bronchial mucus in the lung tissue, alveolar wall thickening, and a large number of infiltrated inflammatory cells in the lungs of rats in the model group. Pathological examination of the kidneys revealed that, in the normal group, renal structure was normal, renal tubular epithelial cells were intact, and interstation was minimal. Inflammatory cell infiltration was observed in the model group. Additionally, glomerular volume was increased and renal tubular epithelial cells were edematous. The results also showed improvement in visceral morphology to various extents in the

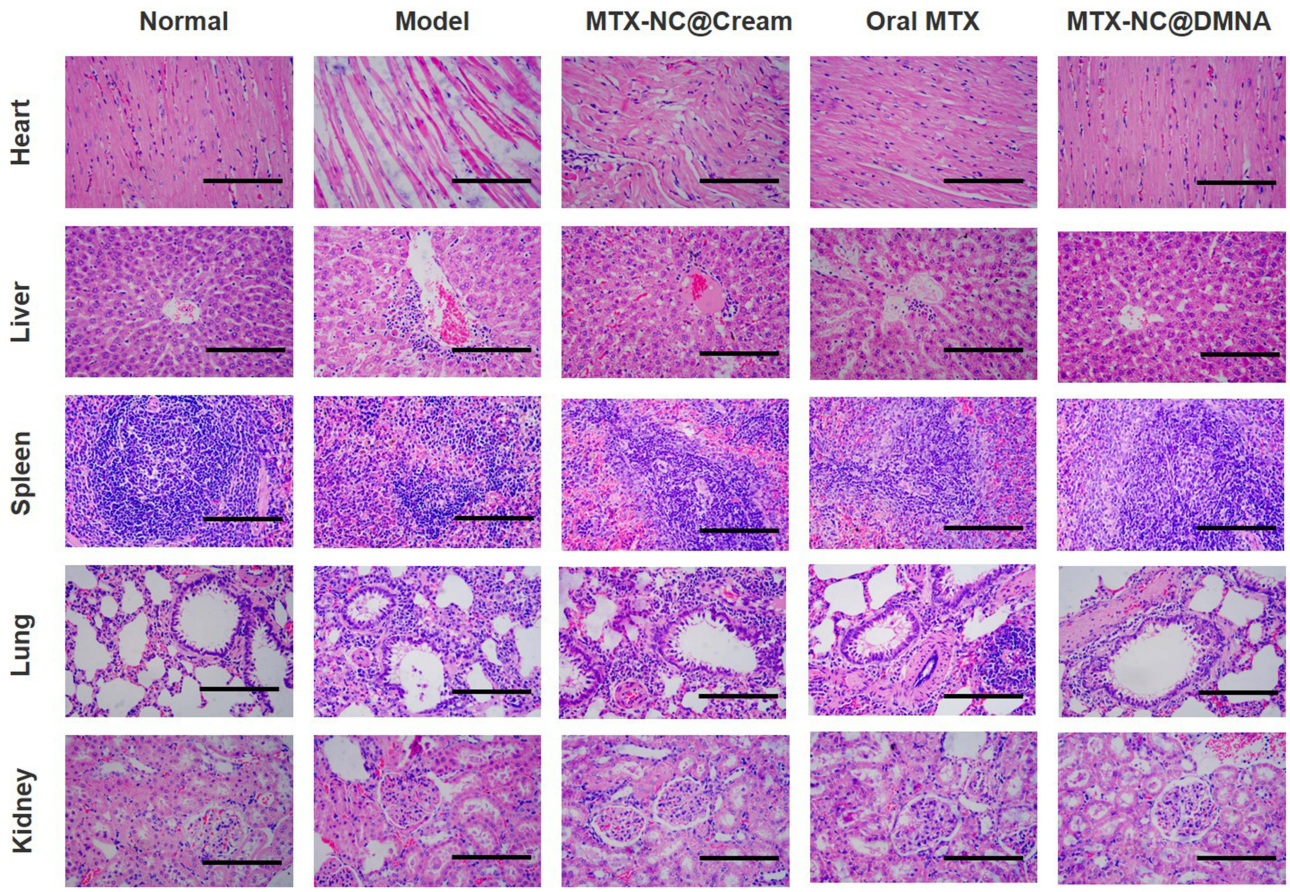

Figure 6 Safety evaluation. H&E staining of major organs in the different groups. Scale bar = 50 μm.
Abbreviation: H&E, hematoxylin and eosin.

rats treated with MTX formulations; however, the MTX-NC@DMNA group showed the highest improvement, which was close to normalization. This indicates that the safety of MTX-NC@DMNA was the highest among the different test formulations.

Conclusion

In this study, we developed a novel DMNA delivery system loaded with MTX-NCs for the treatment of RA. MTX-NCs with carrier-free and surfactant-free helped to improve MTX solubility greatly and effectively avoid carrier- and surfactant-related toxic effects. MTX-NC@DMNA can effectively delivery drug at the site of administration to improve RA treatment and reduce toxicity to major organs. Transdermal MTX delivery with MTX-NC@DMNA has considerable advantages over traditional MTX administration. MTX-NC@DMNA showed good prospects in this study, which make it a potential alternative formulation for the treatment of RA.

Acknowledgments

The authors would like to thank the Natural Science Foundation of Anhui Province (2108085MH317), Key Project of Excellent Youth Talent Support Program in Colleges and Universities of Anhui Province (gxyqZD2020026), University Natural Science Research Key Project of Anhui Province (KJ2021A0812) and Scientific Research Innovation Projects of Bengbu Medical College of Anhui Province (Byycx20034) for the financial support.

Disclosure

The authors report no conflicts of interest in this work.

References

1. Symmons DP. Looking back: rheumatoid arthritis–aetiology, occurrence and mortality. *Rheumatology*. 2005;Suppl 44(suppl_4):iv14–iv17. doi:10.1093/rheumatology/kei055
2. Van der Woude D, Van der Helm-van MA. Update on the epidemiology, risk factors, and disease outcomes of rheumatoid arthritis. *Best Pract Res Clin Rheumatol*. 2018;32(2):174–187. doi:10.1016/j.berh.2018.10.005
3. Colmegna I, Ohata BR, Menard HA. Current understanding of rheumatoid arthritis therapy. *Clin Pharmacol Ther*. 2012;91(4):607–620. doi:10.1038/clpt.2011.325
4. Choi SI, Brahn E. Rheumatoid arthritis therapy: advances from bench to bedside. *Autoimmunity*. 2010;43(7):478–492. doi:10.3109/08916931003674717
5. Kim-Howard XR, Staudt L, James JA. Update in rheumatoid arthritis therapy. *J Okla State Med Assoc*. 2005;98(2):53–62.
6. Abbasi M, Mousavi M J, Jamalzehi S, et al. Strategies toward rheumatoid arthritis therapy; the old and the new. *J Cell Physiol*. 2019;234(7):10018–10031. doi:10.1002/jcp.27860
7. Fraenkel L, Bathon J M, England BR, et al. 2021 American college of rheumatology guideline for the treatment of rheumatoid arthritis. *Arthritis Care Res*. 2021;73(7):924–939. doi:10.1002/acr.24596
8. Fu Q, Feng P, Sun LY, et al. A double-blind, double-dummy, randomized controlled, multicenter trial of 99Tc-methylene diphosphonate in patients with moderate to severe rheumatoid arthritis. *Chin Med J*. 2021;134(12):1457–1464. doi:10.1097/CM9.0000000000001527
9. Olofsson T, Wallman JK, Joud A, et al. Pain over two years after start of biologic versus conventional combination treatment in early rheumatoid arthritis: results from a Swedish randomized controlled trial. *Arthritis Care Res*. 2021;73(9):1312–1321. doi:10.1002/acr.24264
10. Emery P, Tanaka Y, Cardillo T, et al. Temporary interruption of baricitinib: characterization of interruptions and effect on clinical outcomes in patients with rheumatoid arthritis. *Arthritis Res Ther*. 2020;22(1):115. doi:10.1186/s13075-020-02199-8
11. Bianchi G, Caporali R, Todoerti M, et al. Methotrexate and rheumatoid arthritis: current evidence regarding subcutaneous versus oral routes of administration. *Adv Ther*. 2016;33(3):369–378. doi:10.1007/s12325-016-0295-8
12. Vena GA, Cassano N, Iannone F. Update on subcutaneous methotrexate for inflammatory arthritis and psoriasis. *Ther Clin Risk Manag*. 2018;14:105–116. doi:10.2147/TCRM.S154745
13. Jay R. Methotrexate revisited: considerations for subcutaneous administration in RA. *Clin Rheumatol*. 2015;34(2):201–205. doi:10.1007/s10067-014-2830-9
14. Hugle B. MTX intolerance in children and adolescents with juvenile idiopathic arthritis. *Z Rheumatol*. 2019;78(7):620–626. doi:10.1007/s00393-019-0644-5
15. Artacho A, Isaac S, Nayak R, et al. The pretreatment gut microbiome is associated with lack of response to methotrexate in new-onset rheumatoid arthritis. *Arthritis Rheumatol*. 2021;73(6):931–942. doi:10.1002/art.41622
16. Jekic B, Lukovic L, Bunjevacki V, et al. Association of the TYMS 3G/3G genotype with poor response and GGH 354GG genotype with the bone marrow toxicity of the methotrexate in RA patients. *Eur J Clin Pharmacol*. 2013;69(3):377–383. doi:10.1007/s00228-012-1341-3
17. Tu X, Chen R, Huang G, et al. Factors predicting severe myelosuppression and its influence on fertility in patients with low-risk gestational trophoblastic neoplasia receiving single-agent methotrexate chemotherapy. *Cancer Manag Res*. 2020;12:4107–4116. doi:10.2147/CMAR.S252664

18. Nakafero G, Grainge MJ, Card T, et al. What is the incidence of methotrexate or leflunomide discontinuation related to cytopenia, liver enzyme elevation or kidney function decline? *Rheumatology*. 2021;60(12):5785–5794. doi:10.1093/rheumatology/keab254
19. Pivovarov K, Zipursky JS. Low-dose methotrexate toxicity. *CMAJ*. 2019;191(15):E423. doi:10.1503/cmaj.181054
20. Alfaro-Lara R, Espinosa-Ortega HF, Arce-Salinas CA. Systematic review and meta-analysis of the efficacy and safety of leflunomide and methotrexate in the treatment of rheumatoid arthritis. *Reumatol Clín*. 2019;15(3):133–139. doi:10.1016/j.reuma.2017.07.020
21. Blair HA, Deeks ED. Abatacept: a review in rheumatoid arthritis. *Drugs*. 2017;77(11):1221–1233. doi:10.1007/s40265-017-0775-4
22. Kerschbaumer A, Sepriano A, Smolen JS, et al. Efficacy of pharmacological treatment in rheumatoid arthritis: a systematic literature research informing the 2019 update of the EULAR recommendations for management of rheumatoid arthritis. *Ann Rheum Dis*. 2020;79:744–759. doi:10.1136/annrheumdis-2019-216656
23. Salliot C, van der Heijde D. Long-term safety of methotrexate monotherapy in patients with rheumatoid arthritis: a systematic literature research. *Ann Rheum Dis*. 2009;68(7):1100–1104. doi:10.1136/ard.2008.093690
24. W LJ, Choi SO, Felner EI, et al. Dissolving microneedle patch for transdermal delivery of human growth hormone. *Small*. 2011;7(4):531–539. doi:10.1002/smll.201001091
25. Li Y, Hu X, Dong Z, et al. Dissolving microneedle arrays with optimized needle geometry for transcutaneous immunization. *Eur J Pharm Sci*. 2020;151:105361. doi:10.1016/j.ejps.2020.105361
26. Hao Y, Li W, Zhou X, et al. Microneedles-based transdermal drug delivery systems: a review. *J Biomed Nanotechnol*. 2017;13(12):1581–1597. doi:10.1166/jbn.2017.2474
27. Yang H, Wu X, Zhou Z, et al. Enhanced transdermal lymphatic delivery of doxorubicin via hyaluronic acid based transfersomes/microneedle complex for tumor metastasis therapy. *Int J Biol Macromol*. 2019;125:9–16. doi:10.1016/j.ijbiomac.2018.11.230
28. Lopez-Ramirez MA, Soto F, Wang C, et al. Built-in active microneedle patch with enhanced autonomous drug delivery. *Adv Mater*. 2020;32(1): e1905740. doi:10.1002/adma.201905740
29. Karadag A, Ozcelik B, Huang Q. Quercetin nanosuspensions produced by high-pressure homogenization. *J Agric Food Chem*. 2014;62 (8):1852–1859. doi:10.1021/jf404065p
30. Pardhi VP, Verma T, Flora S, et al. Nanocrystals: an overview of fabrication, characterization and therapeutic applications in drug delivery. *Curr Pharm Des*. 2018;24(43):5129–5146. doi:10.2174/1381612825666190215121148
31. Shah R, Soni T, Shah U, et al. Formulation development and characterization of lumefantrine nanosuspension for enhanced antimalarial activity. *J Biomater Sci Polym Ed*. 2021;32(7):833–857. doi:10.1080/09205063.2020.1870378
32. Goel S, Sachdeva M, Agarwal V. Nanosuspension technology: recent patents on drug delivery and their characterizations. *Recent Pat Drug Deliv Formul*. 2019;13(2):91–104. doi:10.2174/1872211313666190614151615
33. Chan KH, Lee WH, Ni M, et al. C-Terminal residue of ultrashort peptides impacts on molecular self-assembly, hydrogelation, and interaction with small-molecule drugs. *Sci Rep*. 2018;8(1). doi:10.1038/s41598-018-35431-2.
34. Gigliobianco MR, Casadidio C, Censi R, et al. Nanocrystals of poorly soluble drugs: drug bioavailability and physicochemical stability. *Pharmaceutics*. 2018;10(3):134. doi:10.3390/pharmaceutics10030134
35. Dos SA, Carvalho FC, Teixeira DA, et al. Computational and experimental approaches for development of methotrexate nanosuspensions by bottom-up nanoprecipitation. *Int J Pharm*. 2017;524(1–2):330–338. doi:10.1016/j.ijpharm.2017.03.068